No effect in primary stability after increasing interference fit in cementless TKA tibial components

Esther Sánchez [a,*], Christoph Schilling [b], Thomas M. Grupp [b,c], Alexander Giurea [d], Nico Verdonschot [a,e], Dennis Janssen [a]

[a] Radboud University Medical Center, Radboud Institute for Health Sciences, Orthopaedic Research Lab, Nijmegen, the Netherlands
[b] Aesculap AG, Research & Development, Tuttlingen, Germany
[c] Ludwig Maximilians University Munich, Department of Orthopaedic Surgery, Physical Medicine & Rehabilitation, Campus Grosshadern, Munich, Germany
[d] Medical University of Vienna, Department of Orthopedics, Vienna, Austria
[e] University of Twente, Laboratory for Biomechanical Engineering, Faculty of Engineering Technology, Enschede, the Netherlands

ARTICLE INFO

ABSTRACT

Cementless total knee arthroplasty (TKA) implants rely on interference fit to achieve initial stability. However, the optimal interference fit is unknown. This study investigates the effect of using different interference fit on the initial stability of tibial TKA implants. Experiments were performed on human cadaveric tibias using a low interference fit of 350 μm of a clinically established cementless porous-coated tibial implant and a high interference fit of 700 μm. The Orthoload peak loads of gait and squat were applied to the specimens with a custom-made load applicator. Micromotions and gaps opening/closing were measured at the bone-implant interface using Digital Image Correlation (DIC) in 6 regions of interest (ROIs). Two multilevel linear mixed-effect models were created with micromotions and gaps as dependent variables. The results revealed no significant differences for micromotions between the two interference fits (gait p = 0.755, squat p = 0.232), nor for gaps opening/ closing (gait p = 0.474, squat p = 0.269). In contrast, significant differences were found for the ROIs in the two dependent variables (p < 0.001), where more gap closing was seen in the posterior ROIs than in the anterior ROIs during both loading configurations. This study showed that increasing the interference fit from 350 to 700 μm did not influence initial stability.

1. Introduction

Total knee arthroplasty (TKA) is the most common and successful surgical procedure to treat osteoarthritis (OA), offering pain relief, improvement of knee function, and providing a better quality of life for patients (Bellemans et al., 2005). However, as the number of TKAs increases, so do revision surgeries due to failure, with aseptic loosening being the most frequent indication (29.8%) (Khan et al., 2016; Singh et al., 2019). There is also an increased incidence in younger patients (< 65 years) receiving TKAs, who tend to have higher activity levels and more demanding lifestyles (Aggarwal et al., 2014). According to implant registries (Khan et al., 2016; National Joint Registry for England, Wales, 2019), younger patients have around 2.5 times higher risk of revision compared to older patients. Moreover, tibial components are considered the weak link of the TKA and show more loosening than femoral components (Crook et al., 2017; Dyrhovden et al., 2017; Napier et al., 2018).

The bone in the proximal tibia is responsible for the mechanical support of the tibial component, where good initial stability is a prerequisite for successful long-term performance (Gao et al., 2019). The tibial baseplate is partially in contact with cortical and trabecular bone and transfers mainly axial compressive forces while the tibial stem & winglets transfer axial and shear forces along with bending loads through the trabecular bone (Ponziani et al., 2017). Previous studies have shown a clear relationship between bone mineral density (BMD) and tibial component migration, where patients with higher BMD showed less migration of the tibial component (Petersen et al., 1999). This suggests that good bone quality contributes to implant fixation (Li and Nilsson, 2000).

The press-fit fixation of tibial components is mainly achieved by the contact of the implant stem & winglets with the trabecular bone. During implantation, the tibial cavity is prepared to be slightly smaller than the external dimensions of the implant stem & winglets. This difference in

---

dimensions between the bone and the implant, known as interference fit (Campi et al., 2018), may affect the initial stability (Gao et al., 2019; Shirazi-Adl et al., 1993). The frictional properties between the bone and the surface coating can also affect primary stability.

Primary stability can be investigated by quantifying micromotions at the bone-implant interface. Animal studies have shown bone ingrowth at the interface when micromotions are < 40 μm, but when micromotions > 150 μm can lead to fibrous tissue formation, compromising the primary stability (Bragdon et al., 1996). Furthermore, the implant does not always fully match the bone surface prepared during surgery, causing gaps at the bone-implant interface. It has been shown that bone can bridge interfacial gaps up to around 2 mm (Goodman et al., 2013). These gaps may not be constant, as they might be considerably affected by the dynamic loads applied during daily activities. Hence, these dynamic gaps may jeopardize ingrowth and secondary stabilization of the implant.

The amount of interference fit can potentially improve primary stability by providing a more reliable press-fit fixation. However, the optimal amount of interference is still unknown. If the interference fit is too low, it may lead to insufficient primary stability and cause migration, loosening, and implant failure. In contrast, a higher interference fit could cause large bone stresses that could lead to bone abrasion during implantation, permanent bone deformation and local fractures, and necrosis after surgery (Campi et al., 2018). Therefore, the purpose of this study was to investigate the effect on the primary stability of increasing the interference fit from 350 μm of a clinically established (Lass et al., 2013; Sampath et al., 2009) knee design to 700 μm by measuring the bone-implant interface micromotions and gaps opening/closing when subjected to two loading conditions. In addition, the influence of bone quality, loading configuration (gait and squat), and regions of interest (ROIs) on the primary stability were evaluated.

2. Material and methods

2.1. Specimen preparation

First, six pairs of relatively young cadaver donor knees (< 60 years old) were selected to enable bones with good bone quality and to ensure a realistic experimental comparison to the clinical situation. After dissection, an experienced surgeon (AG) performed the tibial cuts and implantation according to surgical guidelines. Then, two cementless e. motion® tibial components designs (e.motion® Knee System; Aesculap Tuttlingen, Germany; Fig. 1) with different coating thickness and surface coating were implanted in each pair of fresh-frozen human cadaver tibias (Table 1).

The right tibias were implanted with low interference fit components with a 350 μm coating thickness and a standard Plasmapore® surface coating, while the left tibias were implanted with high interference fit components with a 700 μm coating thickness. This thicker coating was achieved by prolonging the standard coating procedure, which also led

Table 1

Specimen details for age, Body Mass Index (BMI), sex, implant size used, and the loading forces for gait and squat.

Specimen number	Age	BMI	Sex	Implant size	Load Gait (N)	Load squat (N)
1	57	28.74	M	6	2718	2684
2	60	23.4	F	4	1725	1703
3	60	30.38	F	4	2300	2271
4	59	30.89	F	4	2143	2116
5	47	28.49	F	4	1960	1935
6	50	36.31	F	3	2430	2400
	55 ± 5	30 ±4				

The last row shows the average ±SD of age and BMI of the cadaver specimens.

to changes in surface characteristics. As a result, the high interference fit implants had a larger grain morphology with a higher roughness (Ra = 52.21 ± 6.83 μm vs 41.51 ± 0.99 μm) and a slightly higher dynamic coefficient of friction (0.85 ± 0.15 vs 0.78 ± 0.12). After implantation, the exterior of the specimens was painted with a speckle pattern to facilitate the measurement of bone-implant micromotions and gaps opening/closing. The extensive protocol for preparing the bone specimens before testing has been described previously (Berahmani et al., 2017a; Sánchez et al., 2021).

2.2. Loading conditions

Mechanical experiments were performed in an MTS machine (MTS Systems Corporation, Eden Prairie, Minnesota, USA) with a custom-made load applicator that included a femoral component and a tibial insert that matched the sizes of the tibial implants (Table 1). The load applicator was fixed at 14 degrees of flexion for gait and 92° for squat (Fig. 2A), according to the peak axial forces (Average 75) from the Orthoload database (Bergmann et al., 2014; Bergmann, 2008). The Orthoload loading configuration (Table 1) was adjusted to the cadaver specimen bodyweight (BW). The varus/valgus moment was also integrated into the setup by applying the axial force at a medial offset of 9 mm for gait and 3.6 mm for squat (Halder et al., 2012; Kutzner et al., 2017), while other degrees of freedom were fixed. The femoral condyles of the load applicator were aligned with the deepest point of the tibial insert for both loading configurations.

During preconditioning, the specimens were subjected to cyclic loading for 15 min at 1 Hz, at the same axial force levels as applied during the final experiment (see Table 1), followed by a 15-min resting period. A Digital Image Correlation (DIC)-recording was taken before loading, representing the "unloaded" situation. Then, the specimen-specific load was applied in a quasi-static manner at a rate of 100 N/s. After achieving the full-scale load, another DIC-recording was taken under static conditions, representing the "loaded" situation. This procedure was repeated three times at each measurement location. The

Fig. 1. Tibial components with different interference fits. Due to the adapted production method, the high interference fit implant had a higher roughness and a slightly higher dynamic coefficient of friction.
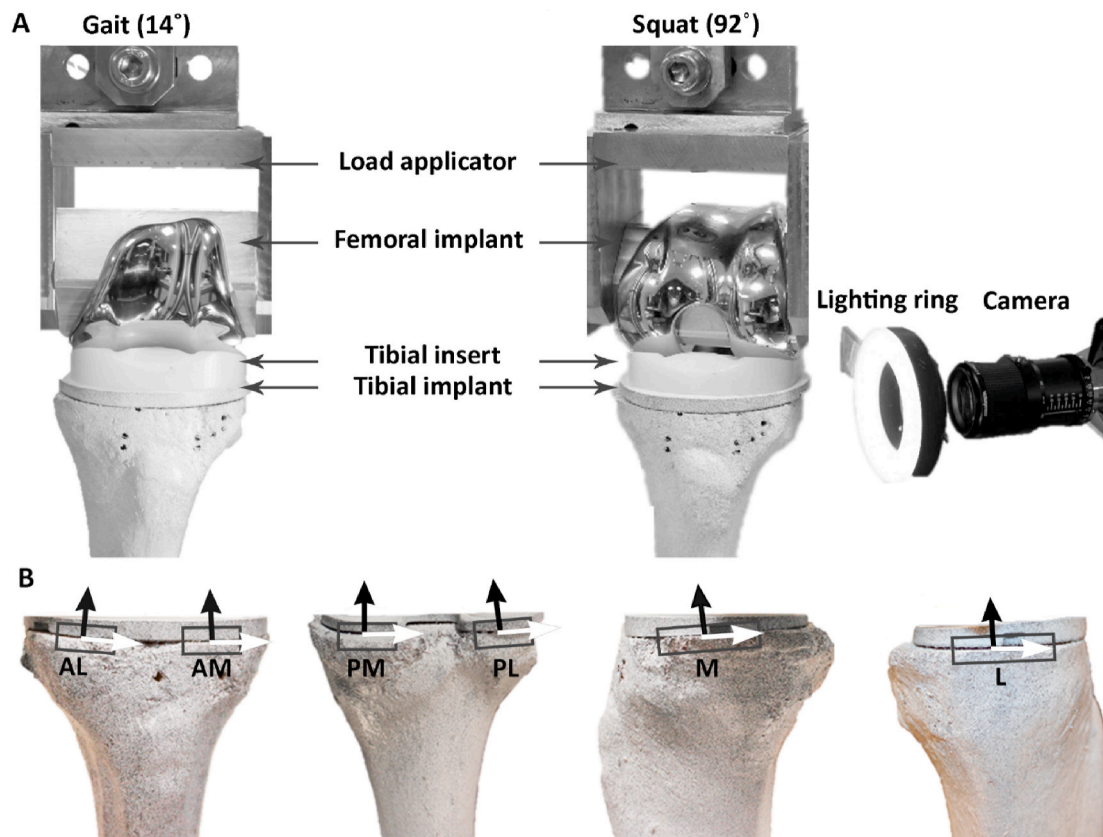
Fig. 2. A) Experimental setup for gait at 14° and squat at 92°. B) The 6 Regions of interest (ROIs) defined at the bone-implant interface for the anterior lateral and medial (AL, AM), posterior medial and lateral (PM, PL), the medial side (M), and lateral side (L). Micromotions are parallel to the interface (white arrows), and gap opening/closing are perpendicular (black arrows).

tibial bones were fixed at the distal end with bone cement (PMMA).

2.3. Micromotion and gap measurements

Relative displacements between bone and implant were measured in six regions of interest (ROIs - Fig. 2B) using DIC. The DIC measurements were performed following a previously developed experimental protocol (Berahmani et al., 2017b), using a resolution of approximately 7.5 μm/pixel. The following six ROIs were defined at the bone-implant interface: anterior lateral (AL), anterior medial (AM), posterior medial (PM), posterior lateral (PL), medial (M), and lateral (L). The position of the DIC system was changed for each specific ROI in order to cover all regions, and the loading-unloading sequence was repeated for each specific ROI.

The relative displacements between the "unloaded" and "loaded" images were determined for each ROI by defining a local coordinate system in the DIC software (GOM Correlate, Freeware, 2017. GOM Inc., Braunschweig, Germany) based on the interface orientation. Within this coordinate system, micromotions were quantified as the shear components of the relative displacements, while gaps motions as the normal components (Fig. 2B). Then, the interfacial gaps were classified as opening gaps when the difference between the relative displacements was positive and closing gaps when the difference was negative. The micromotions and gaps opening/closing for each ROI were averaged for the three repetitions.

2.4. Bone quality measurements

Before cutting the tibial bones and implanting the tibial components, a CT scan (Aquilion ONE GENESIS and VISION, Canon Medical Systems) was used for the bone specimens with a slice thickness of 0.5 mm and a voxel size of 0.39 mm. A calcium hydroxyapatite phantom calibration (Image Analysis, Columbia, KY) was scanned along with each specimen to determine the relationship between calcium values and bone mineral density (BMD) (Keyak et al., 2005). The images obtained from the CT scans were converted to surface meshes (Mimics 20, Materialize, Leuven, Belgium) and subsequently aligned according to the tibial anatomical axis in a Matlab script (Matlab R2019a, The MathWorks, Inc., Natick, Massachusetts, United States). The bone quality was then measured 5 mm below the joint line and using an ROI with a thickness of 10 mm, representing the position of the tibial baseplate on the bone and the area around the tibial stem & winglets (Fig. 3). The average BMD results for each pair of cadaver specimens are given in Table 2.

2.5. Statistical analysis

Two multilevel linear mixed-effect statistical models were created in STATA (Release 16. College Station, TX: StataCorp LLC) with micromotions and gaps opening/closing as dependent variables. The ROIs, BMD, interference fit, and loading configuration were considered independent variables, while cadaver specimens were considered subject factors. A log-transformation was performed in the micromotions results to meet normality, but this was not necessary for the results of the gaps. The models were then divided by loading conditions, and post hoc pairwise comparisons were made to analyze the interaction between all the ROIs. A p-value < 0.05 was considered statistically significant.

3. Results

3.1. Micromotions

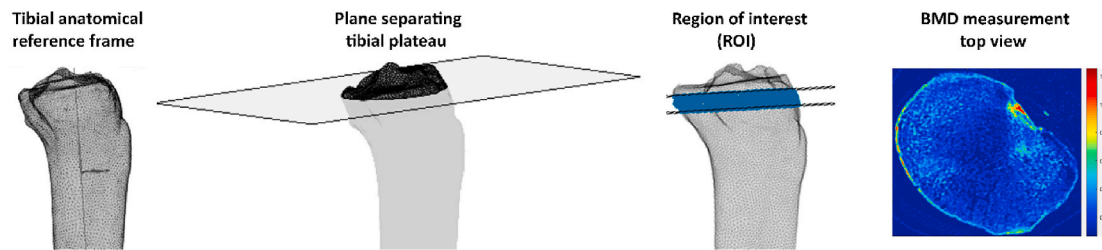Although the mean micromotions results for the high interference fit

Fig. 3. Bone mineral density (BMD) measurements in the proximal tibial bone. The ROI has 10 mm thickness and is 5 mm below the tibial plateau.

Table 2
Bone mineral density (BMD) results for the left and right cadaver specimens; the last row shows the average ±SD.

Specimen number	BMD (G/CM^3) LEFT KNEE	BMD (G/CM^3) RIGHT KNEE
1	0.23	0.22
2	0.16	0.16
3	0.16	0.17
4	0.21	0.21
5	0.27	0.26
6	0.19	0.21
	0.20 ±0.04	**0.21 ± 0.04**

implants were slightly larger compared to the low interference fit implants (Fig. 4A), the results of the statistical model revealed no significant differences between the interference fits in gait (p = 0.755) nor in squat (p = 0.232). In contrast, significant differences were found for the ROIs (p < 0.001), presented in the post hoc analysis.

The post hoc results are shown in Fig. 4B, where the pairwise comparisons between the ROIs are represented as contrasts of predicted marginal means with a 95% confidence interval (CI) for the two interference fit implants. Only the pairwise comparisons different from zero (red line) are statistically significant, represented with blue dots. No significant pairwise comparisons were found during gait since there was only a slight variation in micromotions between the ROIs for both implants. During squat, the comparisons of L vs AL, M vs AL, PM vs AL, and AM vs the rest of the ROIs were significant for the low interference fit implant. In comparison, only PL vs AM and PM vs AM were significant for the high interference fit. Hence, this means that the AM and AL had lower micromotions than the other ROIs in the low interference fit implant, while in the high interference fit only AM showed lower micromotions.

3.2. Interfacial gaps

The mean gaps results are shown in Fig. 5A for the different ROIs. Almost all values were negative, indicating that gap closing occurred upon loading. Except for a small opening motion (positive gap) in the AM ROI for the low interference fit implant during squat. Like the micromotions results, the interference fit did not affect the opening or closing of the gaps, neither in gait (p = 0.474) nor squat (p = 0.269). Moreover, the statistical model results were significant for the ROIs (p < 0.001). During both loading configurations, the posterior ROIs (PL and PM) demonstrated the most substantial amount of closing (average = -151 μm) compared to the anterior ROIs (average = -27 μm).

In the post hoc analysis (Fig. 5B), most of the pairwise comparisons between ROIs were statistically significant, except for the comparisons within the two anterior, the two posterior, and lateral-medial ROIs. Furthermore, PL vs AL, PM vs AL, M vs AM, PL vs AM, PM vs AM, and PM vs L comparisons were significant for the two loading conditions and interference fits. This showed a higher contrast in the opening and closing gaps between the ROIs, especially in the anterior and posterior ROIs. There were also more significant comparisons for the low interference fit than for the high interference fit due to lower anterior gaps.

3.3. Bone quality

The statistical model showed that bone quality had no significant effect on the primary stability of two interference fit implants (micromotions p = 0.688 and gaps p = 0.455). As shown in Table 2, most of the specimens had similar density values with 0.20 ± 0.04 g/cm^3 (mean ± SD) for the left and 0.21 ± 0.04 g/cm^3 for the right specimens.

4. Discussion

The purpose of the current study was to assess the effect of the size of the interference fit on the primary stability of tibial TKA components. This was done by measuring the micromotions and gaps opening/closing at different ROIs at the bone-implant interface during the peak forces of gait and squat. The results indicate no significant differences in micromotions or gaps between the low (clinically established) and the high interference fit implants. Furthermore, both bone quality and loading configuration did not show an effect on the primary stability of the tibial implants. However, significant differences were found between the defined ROIs.

Remarkably, in this study, squatting did not lead to higher micromotions nor bigger gaps than gait. In the Orthoload dataset, the peak axial forces in the superior-inferior (SI) direction were quite similar for both loading configurations. Moreover, the shear forces in the anterior-posterior (AP) and medial-lateral (ML) directions were 10–20 times smaller than the axial loads (Kutzner et al., 2010). It is also likely that the contact point on the tibia was similar during both loading configurations due to the ultra-congruent implant used in the Orthoload dataset, which may influence the AP and ML load transfer (Trepczynski et al., 2019). The e.motion® implant used in our study is also highly congruent, although with a rotating platform bearing. Since no rotational loads were applied, the tibial insert remained at the same position relative to the tibial baseplate during gait and squat. Therefore, the insert position (and coordinate system) is consistent with that of the fixed-bearing implant used in the Orthoload dataset.

Our findings of gaps opening/closing are comparable to another study of a tibial implant with a stem and four pegs during stair descent loads (Bhimji and Meneghini, 2014). They also showed the largest gap closing in the posterior regions, and the lowest closing with even some opening in the anterior regions. Furthermore, another study has a similar implant design as in our study (Yang et al., 2020), where they showed the different parts of the walking and squatting cycle. Considering that the peak axial forces from Orthoload were taken at 50 % of the gait cycle and 70 % of the squat, the results of specimen 3 are comparable to our study with micromotions in the anterior regions below 40 μm during squat. Also, there is some variation of micromotions results between the specimens and the ROIs; however, there was no distinction between shear and normal motions to make a better comparison.

BMD measurements were located at the proximal tibia, considering the position of the implant baseplate on the bone and the interaction between the trabecular bone and the implant stem & winglets due to interference fit. The cadaver specimens appeared to have good bone quality, which may be the result of selecting relatively young cadaver donors (55 ± 5 years), as it is more representative of the indication for
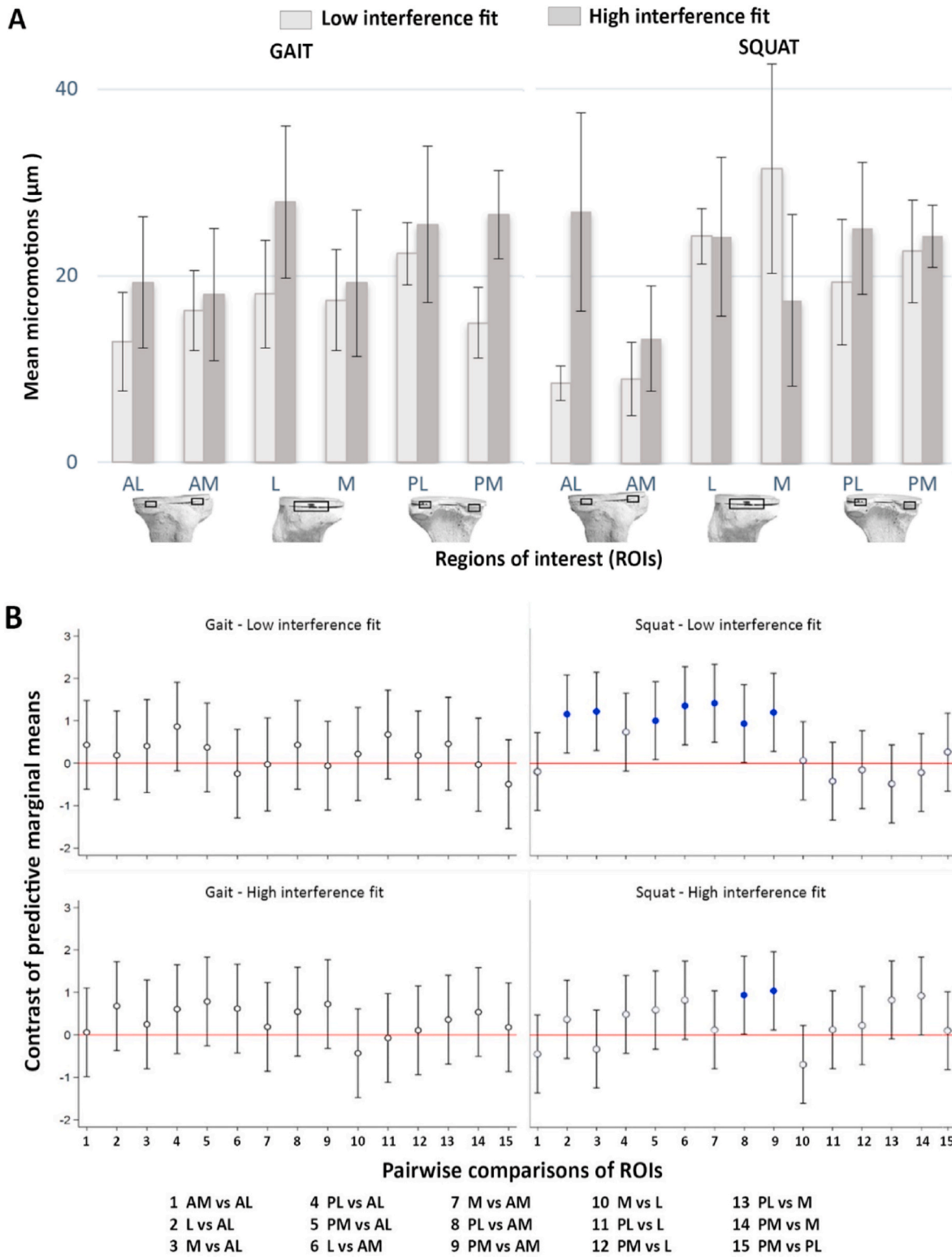
Fig. 4. Low and high interference fit implants results for gait and squat loading. A) Mean micromotions on different ROIs with standard error. B) Contrast of predictive marginal means between ROIs with 95% CI. The blue dots show statistically significant results since they are different from zero; the comparisons passing through zero (red line) are non-significant.

patients with cementless implants. According to another study on femoral components where BMD values were obtained in a similar manner (Berahmani et al., 2015), BMD values < 0.15 g/cm³ could indicate low bone quality, which is lower than was measured in the current tibias. Still, not much information is available on volumetric

values of tibial BMD (Torres-Del-Pliego et al., 2013). Moreover, the limited number of specimens combined with small bone quality variations was not sufficient to demonstrate a relationship between the primary stability of the tibial component and bone quality.

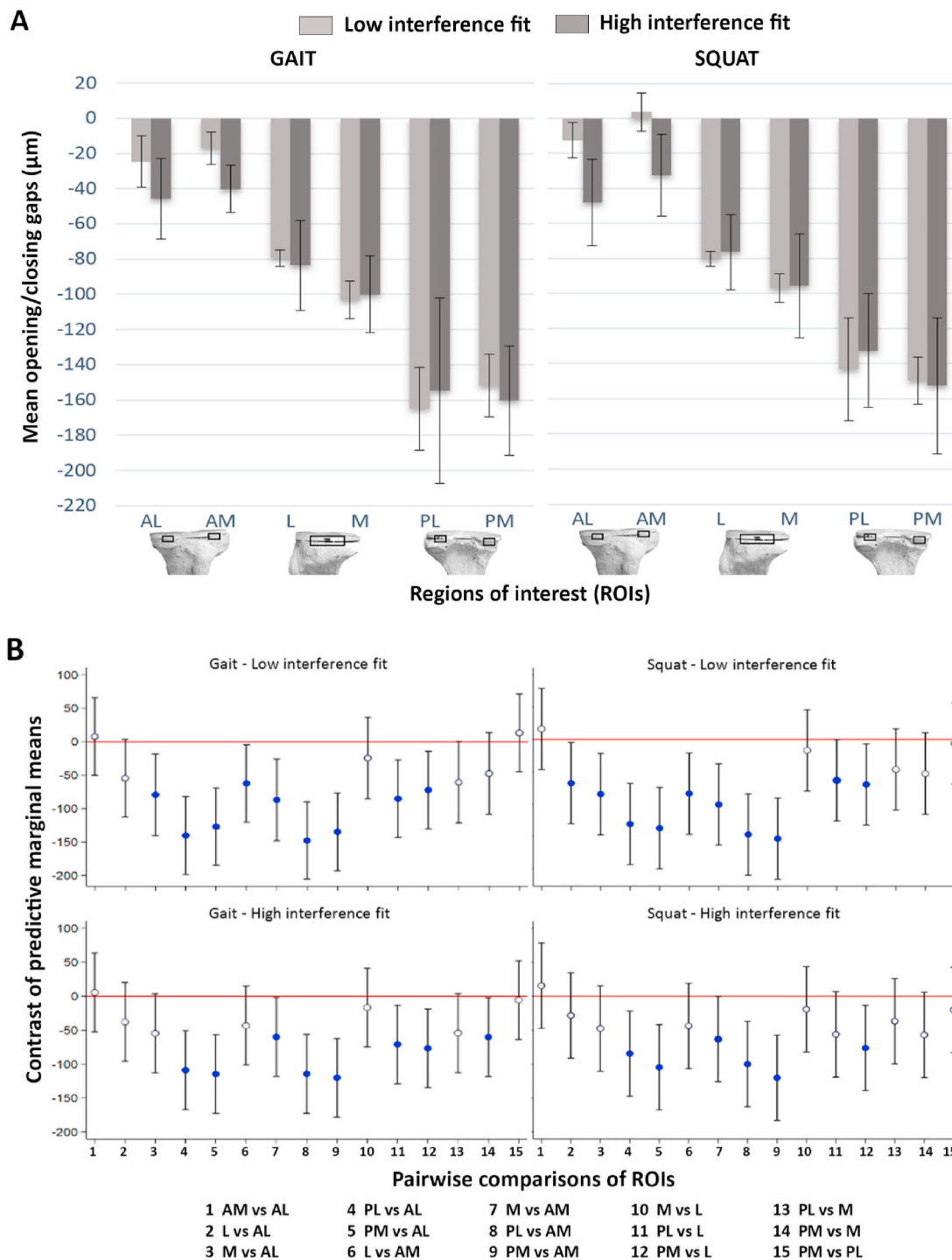In this study, we aimed to investigate the effect of interference fit on

Fig. 5. Low and high interference fit implants results for gait and squat loading. A) Mean gaps opening/closing on different ROIs with standard error. B) Contrast of predictive marginal means between ROIs with 95% CI. The blue dots show statistically significant results since they are different from zero; the comparisons passing through zero (red line) are non-significant.

the primary stability of tibial TKA components. This interference fit can be varied by the manufacturer by adjusting the thickness of the implant coating or downsizing the instrumentation. Intuitively, a higher interference fit should have a better fixation, as it should generate higher compressive stresses and frictional shear forces at the interface. On the other hand, it could also generate more plasticity around the implant, limiting the additional stability. Interestingly, our results did not demonstrate this mechanism. One possible explanation for this discrepancy is that a larger interference fit could cause bone abrasion and permanent bone deformation during implant insertion. As a result,

part of the compressive capacity of the bone is lost during the insertion phase, meaning that the nominal interference fit designed into the system is not the same as the actual interference fit achieved during surgery (Berahmani et al., 2018).

Unfortunately, it was not possible to measure bone damage after implantation without further damaging the bone when extracting the tibial component. In a previous study with press-fit femoral components, we found that the implantation process caused bone damage. The components were removed by cutting the posterior condyles, similarly to another study (Berahmani et al., 2018). Then using HR-pQCT, we

could visualize and quantify the amount of permanent bone deformation. This damage can be quite substantial (up to 1.5 mm) and may depend on the amount of interference fit designed into the system. While for the femoral component, the compressive forces are partially acting on cortical bone. The tibial component relies directly on the contact between the trabecular bone and the tibial stem & winglets, resulting in even more bone abrasion and deformation when inserting the component.

The results of our study showed that micromotions in both tibial components did not exceed the bone ingrowth threshold of 40 μm, suggesting good primary stability that could lead to better long-term stability. The results are also in line with our previous study with press-fit femoral TKA components (Sánchez et al., 2021), which correspond with the clinical results on the e.motion® implant with 350 μm interference fit, where the survival rate was 96.2% for cementless TKA components after 8.3 years postoperatively (Lass et al., 2013). However, the opening and closing motions were larger than the shear micromotions, ranging from practically zero in the anterior regions up to 160 μm in the posterior regions. The exact implications of these motions on bone formation at the interface are uncertain since micromotion thresholds determined in the past were based only on shear motions. Clearly, excessive motions could inhibit osseointegration and secondary fixation, but defining the exact threshold requires further investigation. Nonetheless, considering that the standard interference fit implant has a good clinical track record and the similarity between the outcomes for the two systems, increasing the interference fit to 700 μm can be expected to provide equally good primary stability. Hence, it can be considered as a good range for an interference fit.

4.1. Limitations

The main limitation of our study was the variability between specimens since tibias can vary in size, shape, and material properties depending on patient-related factors such as age, anatomy, and weight (Tissakht et al., 1995). Variability is an inevitable and essential factor to consider when using cadaveric bones as they have non-homogeneous material properties (Han et al., 2020; Yang et al., 2020). It can help to have more realistic results and to evaluate the press-fit fixation of tibial implants. Few studies like this were performed with cadaver bones (Han et al., 2020; Yang et al., 2020), while most previous studies used sawbones specimens (Bhimji and Meneghini, 2012; Luring et al., 2006; Navacchia et al., 2018). There may also be differences in the cut accuracy and the implant position, which we tried to minimize by using one highly experienced surgeon. The implantation of the tibial components was done by mimicking the clinical situation as closely as possible, rather than milling the tibias to exact specifications. Based on visual inspection, all implants were well-seated, although small gaps were seen at the interface in some regions. More importantly, there were no noticeable changes before and after preconditioning, and there were also no remarkable differences between the two implant systems.

Another limitation is the loading condition, as only the peak axial forces from gait and squat were used with an offset that simulated the varus-valgus moment. Additionally, with the absence of the PCL in the cadaver experiment, the loading condition in squat may not have simulated adequate femoral roll-back. It is possible that a more posterior point of load application, and therefore a larger flexion moment, would have altered the anterior opening and closing motions. Another study (Yang et al., 2020), reported substantial motions in the anterior regions (up to 200 μm), while these motions were only found in the posterior regions in our study. This suggests that an additional flexion moment influences the pivot point of the tilting motion of the tibial component under compressive loading. A 3-degree posterior slope was integrated into the implant design, contributing to the AP shear forces. However, the forces from the Orthoload dataset were obtained with a posterior slope of around 7°. Ideally, an implant-specific loading configuration would be derived, and subsequently applied in a testing apparatus with a

6-degree of freedom loading applicator. From a practical point of view, simplifications in loading conditions have to be made in experimental testing conditions. These tests can be used to validate FE models, which are subsequently more suitable to apply and investigate the effect of full loading cycles with all force components involved.

The DIC technique was used to directly measure the micromotions and gaps opening/closing at the bone-implant interface. This technique has the advantage of providing more accurate quantification of micromotions and gaps, compared to studies using linear variable differential transducers (LVDTs) (Bhimji and Meneghini, 2012; Chong et al., 2010; Crook et al., 2017). In addition, we included a distinction between micromotions and gaps, which was not always clear in previous studies. However, our results are measured at specific locations, and it could be that the micromotions and gaps patterns are different at other locations. Again, linking this cadaveric experiment with FE analyses may allow assessing micromotions and gaps along the whole bone-implant interface.

4.2. Conclusion

The results presented here demonstrate that, in this experimental setup, increasing the interference fit from 350 μm (clinically established design) to 700 μm does not affect the primary stability at the bone-implant interface of tibial TKA. While micromotions values were all below the threshold allowing bone ingrowth, the dynamic gaps at the interface were quite substantial, especially in the posterior ROIs. Since this type of implant has given satisfactory clinical results, it can be expected that the results of gaps opening/closing were also under a threshold that can guarantee good primary stability. Hence, an interference fit of 700 μm can be considered an adequate range for press-fit fixation for this type of implant.

Credit author statement

Esther Sánchez: Conceptualization, Methodology, Software, Validation, Formal analysis, Investigation, Writing - original draft, Visualization, Project administration. **Christoph Schilling:** Conceptualization, Resources, Writing - review & editing, Supervision, Funding acquisition. **Thomas M. Grupp:** Conceptualization, Resources, Writing - review & editing, Supervision, Funding acquisition. **Alexander Giurea:** Resources, Writing - review & editing. **Nico Verdonschot:** Conceptualization, Methodology, Validation, Resources, Writing - review & editing, Supervision. **Dennis Janssen:** Conceptualization, Methodology, Validation, Resources, Writing - review & editing, Supervision, Project administration.

project.

References

Aggarwal, V.K., Goyal, N., Deirmengian, G., Rangavajulla, A., Parvizi, J., Austin, M.S., 2014. Revision total knee arthroplasty in the young patient: is there trouble on the horizon? J. Bone Jt. Surg. - Ser. A 96, 536–542. https://doi.org/10.2106/JBJS.M.00131.

Bellemans, J., Ries, M.D., Victor, J.M.K., 2005. Total Knee Arthoplasty: A Guide to Get Better Performance. Springer S.

Bergmann, G. (Ed.), 2008. Charité Universitaetsmedizin Berlin. OrthoLoad. Feb. 1, 2018.

Berahmani, S., Hendriks, M., de Jong, J.J.A., van den Bergh, J.P.W., Maal, T., Janssen, D., Verdonschot, N., 2018. Evaluation of interference fit and bone damage of an uncemented femoral knee implant. Clin. Biomech. 51, 1–9. https://doi.org/10.1016/j.clinbiomech.2017.10.022.

Berahmani, S., Hendriks, M., Wolfson, D., Wright, A., Janssen, D., Verdonschot, N., 2017a. Experimental pre-clinical assessment of the primary stability of two cementless femoral knee components. J. Mech. Behav. Biomed. Mater. 75, 322–329. https://doi.org/10.1016/j.jmbbm.2017.07.043.

Berahmani, S., Janssen, D., Verdonschot, N., 2017b. Experimental and computational analysis of micromotions of an uncemented femoral knee implant using elastic and plastic bone material models. J. Biomech. 61, 137–143. https://doi.org/10.1016/j.jbiomech.2017.07.023.

Berahmani, S., Janssen, D., Wolfson, D., Rivard, K., de Waal Malefijt, M., Verdonschot, N., 2015. The effect of surface morphology on the primary fixation strength of uncemented femoral knee prosthesis: a cadaveric study. J. Arthroplasty 30, 300–307. https://doi.org/10.1016/j.arth.2014.09.030.

Bergmann, G., Bender, A., Graichen, F., Dymke, J., Rohlmann, A., Trepczynski, A., Heller, M.O., Kutzner, I., 2014. Standardized loads acting in kne implants. PLoS One 9. https://doi.org/10.1371/journal.pone.0155612.

Bhimji, S., Meneghini, R.M., 2014. Micromotion of cementless tibial baseplates: keels with adjuvant pegs offer more stability than pegs alone. J. Arthroplasty 29, 1503–1506. https://doi.org/10.1016/j.arth.2014.02.016.

Bhimji, S., Meneghini, R.M., 2012. Micromotion of cementless tibial baseplates under physiological loading conditions. J. Arthroplasty 27, 648–654. https://doi.org/10.1016/j.arth.2011.06.010.

Bragdon, C.R., Burke, D., Lowenstein, J.D., Connor, D.O.O., Ramamurti, B., Jasty, M., Harris, W.H., 1996. Differences in stiffness between a cementless and cancellous bone into varying amounts of the interface porous implant vivo in dogs due implant motion. Clin. Orthop. 11, 945–951.

Campi, S., Mellon, S.J., Ridley, D., Foulke, B., Dodd, C.A.F., Pandit, H.G., Murray, D.W., 2018. Optimal interference of the tibial component of the cementless oxford unicompartmental knee replacement. Bone Joint Res. 7, 226–231. https://doi.org/10.1302/2046-3758.73.BJR-2017-0193.R1.

Chong, D.Y.R., Hansen, U.N., Amis, A.A., 2010. Analysis of bone-prosthesis interface micromotion for cementless tibial prosthesis fixation and the influence of loading conditions. J. Biomech. 43, 1074–1080. https://doi.org/10.1016/j.jbiomech.2009.12.006.

Crook, P.D., Owen, J.R., Hess, S.R., Al-Humadi, S.M., Wayne, J.S., Jiranek, W.A., 2017. Initial stability of cemented vs cementless tibial components under cyclic load. J. Arthroplasty 32, 2556–2562. https://doi.org/10.1016/j.arth.2017.03.039.

Dyrhovden, G.S., Lygre, S.H.L., Badawy, M., Gøthesen, Ø., Furnes, O., 2017. Have the causes of revision for total and unicompartmental knee arthroplasties changed during the past two decades? Clin. Orthop. Relat. Res. 475, 1874–1886. https://doi.org/10.1007/s11999-017-5316-7.

Gao, X., Fraulob, M., Haïat, G., 2019. Biomechanical behaviours of the bone–implant interface: a review. J. R. Soc. Interface 16, 20190259. https://doi.org/10.1098/rsif.2019.0259.

Goodman, S.B., Yao, Z., Keeney, M., Yang, F., 2013. The future of biologic coatings for orthopaedic implants. Biomaterials 34, 3174–3183. https://doi.org/10.1016/j.biomaterials.2013.01.074.

Halder, A., Kutzner, I., Graichen, F., Heinlein, B., Beier, A., Bergmann, G., 2012. Influence of limb alignment on mediolateral loading in total knee replacement. J. Bone Jt. Surg. Am. 94, 1023–1029. https://doi.org/10.2106/JBJS.K.00927.

Han, S., Patel, R.V., Ismaily, S.K., Jones, H.L., Gold, J.E., Noble, P.C., 2020. Micromotion and migration of cementless tibial trays under functional loading conditions. J. Arthroplasty 36, 349–355. https://doi.org/10.1016/j.arth.2020.07.017.

Keyak, J.H., Kaneko, T.S., Tehranzadeh, J., Skinner, H.B., 2005. Predicting proximal femoral strength using structural engineering models. Clin. Orthop. Relat. Res. 219–228. https://doi.org/10.1097/01.blo.0000164400.37905.22.

Khan, M., Osman, K., Green, G., Haddad, F.S., 2016. The epidemiology of failure in total knee arthroplasty. Bone Joint Lett. J 98-B, 105–112. https://doi.org/10.1302/0301-620X.98B1.36293.

Kutzner, I., Bender, A., Dymke, J., Duda, G., Von Roth, P., Bergmann, G., 2017. Mediolateral force distribution at the knee joint shifts across activities and is driven by tibiofemoral alignment. Bone Jt. J. 99B, 779–787. https://doi.org/10.1302/0301-620X.99B6.BJJ-2016-0713.R1.

Kutzner, I., Heinlein, B., Graichen, F., Bender, A., Rohlmann, A., Halder, A., Beier, A., Bergmann, G., 2010. Loading of the knee joint during activities of daily living measured in vivo in five subjects. J. Biomech. 43, 2164–2173. https://doi.org/10.1016/j.jbiomech.2010.03.046.

Lass, R., Kubista, B., Holinka, J., Pfeiffer, M., Schuller, S., Stenicka, S., Windhager, R., Giurea, A., 2013. Comparison of cementless and hybrid cemented total knee arthroplasty. Orthopedics 36, e420–e427. https://doi.org/10.3928/01477447-20130327-16.

Li, M.G., Nilsson, K.G., 2000. The effect of the preoperative bone quality on the fixation of the tibial component in total knee arthroplasty. J. Arthroplasty 15, 744–753. https://doi.org/10.1054/arth.2000.6617.

Luring, C., Perlick, L., Trepte, C., Linhardt, O., Perlick, C., Plitz, W., Grifka, J., 2006. Micromotion in cemented rotating platform total knee arthroplasty: cemented tibial stem versus hybrid fixation. Arch. Orthop. Trauma Surg. 126, 45–48. https://doi.org/10.1007/s00402-005-0082-5.

Napier, R.J., O'Neill, C., O'Brien, S., Doran, E., Mockford, B., Boldt, J., Beverland, D.E., 2018. A prospective evaluation of a largely cementless total knee arthroplasty cohort without patellar resurfacing: 10-year outcomes and survivorship. BMC Muscoskel. Disord. 19, 1–9. https://doi.org/10.1186/s12891-018-2128-1.

National Joint Registry for England, Wales, N.I. and the I. of M, 2019. 16th Annual Report 2019.

Navacchia, A., Clary, C.W., Wilson, H.L., Behnam, Y.A., Rullkoetter, P.J., 2018. Validation of model-predicted tibial tray-synthetic bone relative motion in cementless total knee replacement during activities of daily living. J. Biomech. 77, 115–123. https://doi.org/10.1016/j.jbiomech.2018.06.024.

Petersen, M.M., Nielsen, P.T., Lebech, A., Toksvig-Larsen, S., Lund, B., 1999. Preoperative bone mineral density of the proximal tibia and migration of the tibial component after uncemented total knee arthroplasty. J. Arthroplasty 14, 77–81. https://doi.org/10.1016/S0883-5403(99)90206-1.

Ponziani, L., Di Caprio, F., Meringolo, R., 2017. Cementless knee arthroplasty. Acta Biomed. 88, 11–18. https://doi.org/10.23750/abm.v88i4-S.6789.

Sampath, S.A.C., Voon, S.H., Sangster, M., Davies, H., 2009. The statistical relationship between varus deformity, surgeon's experience, BMI and tourniquet time for computer assisted total knee replacements. Knee 16, 121–124. https://doi.org/10.1016/j.knee.2008.09.008.

Sánchez, E., Schilling, C., Grupp, T.M., Giurea, A., Wyers, C., van den Bergh, J., Verdonschot, N., Janssen, D., 2021. The effect of different interference fits on the primary fixation of a cementless femoral component during experimental testing. J. Mech. Behav. Biomed. Mater. 113 https://doi.org/10.1016/j.jmbbm.2020.104189.

Shirazi-Adl, A., Dammak, M., Paiement, G., 1993. Experimental determination of friction characteristics at the trabecular bone/porous-coated metal interface in cementless implants. J. Biomed. Mater. Res. 27, 167–175. https://doi.org/10.1002/jbm.820270205.

Singh, J.A., Yu, S., Chen, L., Cleveland, J.D., 2019. Rates of total joint replacement in the United States: future projections to 2020–2040 using the national inpatient sample. J. Rheumatol. 46, 1134–1140. https://doi.org/10.3899/jrheum.170990.

Tissakht, M., Eskandari, H., Ahmed, A.M., 1995. Micromotion analysis of the fixation of total knee tibial component. Comput. Struct. 56, 365–375. https://doi.org/10.1016/0045-7949(95)00029-G.

Torres-Del-Pliego, E., Vilaplana, L., Güerri-Fernández, R., Diez-Pérez, A., 2013. Measuring bone quality. Curr. Rheumatol. Rep. 15 https://doi.org/10.1007/s11926-013-0373-8.

Trepczynski, A., Kutzner, I., Schütz, P., Dymke, J., List, R., von Roth, P., Moewis, P., Bergmann, G., Taylor, W.R., Duda, G.N., 2019. Tibio-femoral contact force distribution is not the only factor governing pivot location after total knee arthroplasty. Sci. Rep. 9, 1–9. https://doi.org/10.1038/s41598-018-37189-z.

Yang, H., Bayoglu, R., Renani, M.S., Behnam, Y., Navacchia, A., Clary, C., Rullkoetter, P.J., 2020. Validation and sensitivity of model-predicted proximal tibial displacement and tray micromotion in cementless total knee arthroplasty under physiological loading conditions. J. Mech. Behav. Biomed. Mater. 109, 103793 https://doi.org/10.1016/j.jmbbm.2020.103793.